Chemistry of Metals and Alloys

Chem. Met. Alloys 12 (2019) 1-8
Ivan Franko National University of Lviv
www.chemetal-journal.org

Structural and electrical characterization of RCu$_5$Sn compounds (R = Y, Gd, Tb, Dy, Ho, Er, and Tm)

I. ROMANIV[1], L. ROMAKA[1]*, B. KUZHEL[1], V.V. ROMAKA[2], M. RUDCHENKO[1], Yu. STADNYK[1], M. KONYK[1], M. RUDKO[3]

[1] *Department of Inorganic Chemistry, Ivan Franko National University of Lviv, Kyryla i Mefodiya St. 6, 79005 Lviv, Ukraine*
[2] *Department of Materials Engineering and Applied Physics, Lviv Polytechnic National University, Ustyyanovycha St. 5, 79013 Lviv, Ukraine*
[3] *Scientific-Technical and Educational Center of Low-Temperature Studies, Ivan Franko National University of Lviv, Dragomanova St. 50, 79005 Lviv, Ukraine*
* *Corresponding author. E-mail: lyubov.romaka@lnu.edu.ua*

Received August 31, 2018; accepted June 18, 2019; available on-line August 16, 2019
https://doi.org/10.30970/cma12.0374

A series of RCu$_5$Sn intermetallic compounds (R = Y, Gd, Tb, Dy, Ho, Er, and Tm) was synthesized from the elements by arc-melting, annealed at 870 K and characterized by X-ray powder diffraction and energy-dispersive X-ray analyses. Rietveld refinements of the crystal structures showed that the compounds crystallize in the structure type CeCu$_5$Au (ordered variant of the CeCu$_6$ type, space group *Pnma*). Measurements of the electrical resistivity indicated metallic type of conductivity for all the studied compounds in the temperature range 11-300 K. Magnetic ordering at low temperature was, when in the temperature range of the measurements, confirmed by the electrical resistivity measurements. Electronic structure calculations performed for YCu$_5$Sn are in good agreement with the electrical transport studies.

Intermetallics / Crystal structure / X-ray diffraction / Electrical properties / DFT modeling

1. Introduction

Investigations of R–Cu–Sn ternary systems (where R is a rare-earth metal) resulted in the identification of several series of isotypic ternary stannides [1,2]. In the Cu-rich part of the R–Cu–Sn systems, two series of ternary compounds were found in the majority of the systems, $R_{1.9}$Cu$_{9.2}$Sn$_{2.8}$ (R = Y, Ce-Sm, Gd-Lu) with hexagonal $R_{1.9}$Cu$_{9.2}$Sn$_{2.8}$-type structure [3] and RCu$_5$Sn (CeCu$_5$Au-type structure), reported for all rare earths except Lu [4,5]. The structures of both the $R_{1.9}$Cu$_{9.2}$Sn$_{2.8}$ and RCu$_5$Sn series are related to the binary CaCu$_5$ type, as they are constructed from the same structural fragments, stacked in different manners. Crystal structure studies of the RCu$_5$Sn stannides where R = La-Gd [6] by single-crystal diffraction confirmed that they belong to the CeCu$_5$Au-type (an ordered ternary variant of the CeCu$_6$-type) [7]. Magnetic property measurements of CeCu$_5$Sn and PrCu$_5$Sn [4,6] indicated antiferromagnetic ordering in CeCu$_5$Sn, while the ground state of PrCu$_5$Sn is non-ordered. Both stannides are characterized by metallic type of conductivity. An investigation of the influence of the Sn-content on the magnetic behavior, within the solid solution CeCu$_{6-x}$Sn$_x$ with CeCu$_6$-type structure, showed a transition from Kondo-like behavior to antiferromagnetic ordering [8]. The magnetic properties of the RCu$_5$Sn intermetallics where R is Gd-Yb, have been studied in the temperature interval from 2 to 300 K [5]. The stannides with R = Gd, Tb, Dy, Ho, and Er showed antiferromagnetic ordering at low temperatures, while TmCu$_5$Sn and YbCu$_5$Sn did not exhibit magnetic ordering down to 2 K. TmCu$_5$Sn is a Curie-Weiss paramagnet with a calculated magnetic moment close to that of free Tm^{3+} ions. YbCu$_5$Sn is characterized by an intermediate valence state of the Yb atoms.

The aim of the present study was to extend the structural studies and determine the electrical resistivity of RCu$_5$Sn stannides, and confront the experimental results with those of DFT modeling.

2. Experimental details

Samples of nominal composition R_{15}Cu$_{70}$Sn$_{15}$ were synthesized by direct arc-melting of the constituent elements (purity of the rare earths 99.9 wt.%, Cu 99.99 wt.%, and Sn 99.999 wt.%) under Ti-gettered argon atmosphere on a water-cooled copper hearth. The overall weight losses after arc-melting were

generally less than 1 wt.%. In the previously studied *R*–Cu–Sn systems, the formation of the RCu$_5$Sn compounds was observed at 670 and 770 K [2]. Taking into account the high Cu content, for the study of the structural and magnetic characteristics of RCu$_5$Sn stannides [5] an annealing temperature of 870 K was chosen for better homogenization of the samples. In the present work the alloys were annealed at the same temperature, 870 K, for 720 h (the time of annealing was determined empirically) in evacuated silica tubes and subsequently quenched in ice water. The prepared samples were examined by X-ray powder diffraction (XRPD; diffractometer DRON-2.0, Fe $K\alpha$ radiation) and Scanning Electron Microscopy (SEM) using a REMMA-102 scanning microscope. Quantitative electron probe microanalysis (EPMA) was carried out by an energy-dispersive X-ray analyzer with the pure elements as standards (*K*- and *L*-lines were used). XRPD data for the crystal structure refinements were collected in the transmission mode on a STOE STADI P powder diffractometer (Cu $K\alpha_1$ radiation, graphite monochromator). Calculation of the lattice parameters and the crystal structure refinements were performed using the WinCSD and FullProf Suite program packages [9,10].

The electrical resistivity was measured in the temperature range 11-300 K, employing the four-probe method on millimeter-scale, well-shaped pieces cut by spark erosion from polycrystalline samples, using a closed-cycle helium cooler (Advanced Research systems, USA).

DFT calculations were carried out with the Elk v4.3.06 package [11], using an all-electron full-potential linearized augmented-plane wave (FP-LAPW) code with Perdew-Burke-Enzerhoff exchange-correlation functional in generalized gradient approximation (GGA) [12]. The *k*-point mesh size was set to 10×10×10, giving in total 216 *k*-points in the irreducible part of the unit cell. Prior to the final total energy calculations, the geometry of the initial structure (lattice vectors and atomic coordinates) was completely relaxed. Proper values of the muffin-tin radii were selected automatically at the initial stage of the calculations. The distribution of the total and partial densities of states (DOS) was calculated by a trilinear method using a 1000 *k*-point grid for integrating functions in the Brillouin zone and 1000 energy points in the DOS plot. The interstitial DOS was included into the total DOS distribution, while the partial DOS for each atom type was obtained only within the volume of the appropriate muffin-tin sphere. Visualization of the volumetric data was carried out with the VESTA package [13].

3. Results and discussion

3.1. Crystal structures

During a study of the Ho–Cu–Sn system, the crystal structure of the HoCu$_5$Sn stannide was refined on X-ray powder diffraction data [14]. According to the refinement this compound belongs to the CeCu$_5$Au type structure (space group *Pnma*, a = 0.81889(7), b = 0.49599(4), c = 1.05652(8) nm) with ordered distribution of the atoms among the crystallographic sites [14]. The results were in a good agreement with the composition of the compound obtained from EPMA data ($Ho_{15.06}Cu_{69.98}Sn_{14.96}$). Structural studies of the DyCu$_5$Sn and TmCu$_5$Sn compounds by single-crystal and powder diffraction were reported in [15,16]; both compounds adopt the CeCu$_5$Au-type.

Earlier refinements of the structures of the Gd and Er compounds [5,17], had revealed slight off-stoichiometery, and it was decided to perform detailed structural studies of these and other representatives of the RCu$_5$Sn series. In the present work complete crystal structure refinements were carried out on samples of nominal composition $Gd_{15}Cu_{70}Sn_{15}$, $Tb_{15}Cu_{70}Sn_{15}$, $Er_{15}Cu_{70}Sn_{15}$, and $Y_{15}Cu_{70}Sn_{15}$ (*i.e.* slightly Cu-deficient with respect to 1:5:1 stoichiometry), using as starting model the structure type CeCu$_5$Au. All the studied compounds were found to crystallize with ordered CeCu$_5$Au-type structures. The final atomic and isotropic displacement parameters are listed in Table 1 and the cell parameters can be found in Table 2. Observed, calculated and difference X-ray patterns of the Tb- and Er-containing samples are shown in Figs. 1,2.

As reported in [5], the RCu$_5$Sn stannides where *R* is a rare-earth of the yttrium group belong to the structure type CeCu$_5$Au (space group *Pnma*), where one of the 4*c* sites is occupied by Au (here Sn). In the model of the CeCu$_5$Au type applied to the RCu$_5$Sn compounds, one crystallographic position (8*d*) may in addition be occupied by a mixture of Cu and Sn atoms. In the case of the stannides with Gd and Er, the earlier crystal structure refinements [5,17] showed a small deviation from 1:5:1 stoichiometry, giving the composition RCu$_{5-x}$Sn$_{1+x}$. According to the refinements performed in this work, the RCu$_5$Sn compounds with CeCu$_5$Au-type structure are characterized by an ordered distribution of the atoms corresponds to the formula RCu$_5$Sn.

3.2. Electrical properties

To study the changes in the electrical properties, a series of RCu$_5$Sn compounds, where *R* stands for Y, Gd-Tm, was prepared and analyzed by X-ray diffraction and electron microprobe analysis. According to the X-ray phase analysis, all the compounds adopt an orthorhombic structure of the CeCu$_5$Au-type. The refined lattice parameters and EPMA data are given in Table 2. As typical examples, SEM pictures of the Ho- and Er-containing samples are shown in Fig. 3.

The temperature dependencies of the electrical resistivity $\rho(T)$ of the RCu$_5$Sn compounds measured in the temperature range 11-300 K are shown in Figs. 4,5.

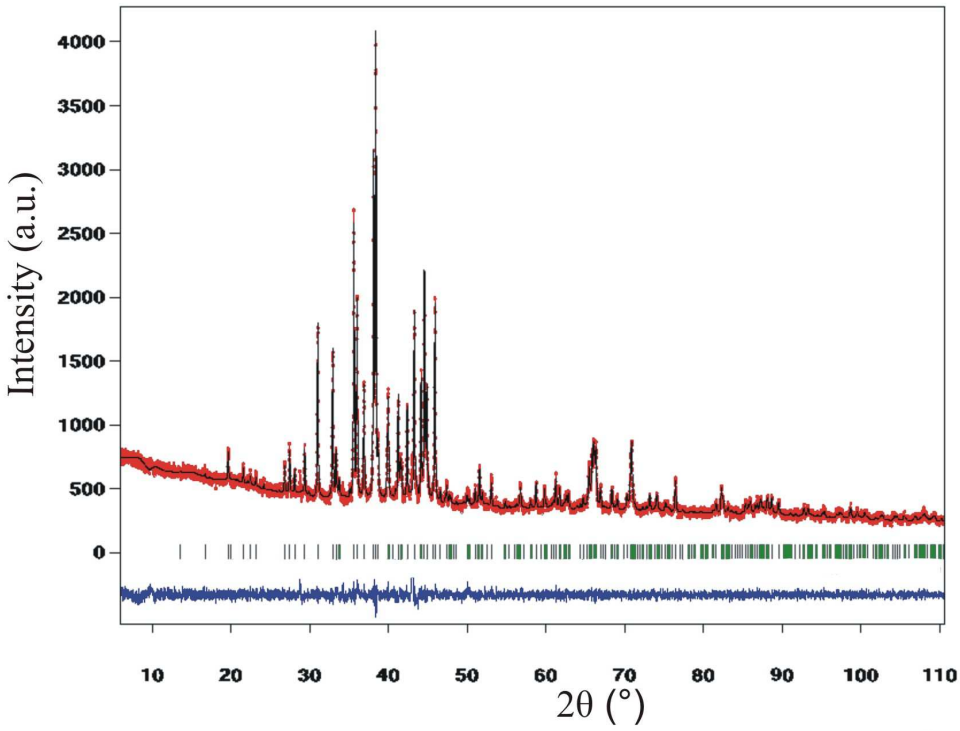

Fig. 1 Observed, calculated and difference X-ray patterns of the $Tb_{15}Cu_{70}Sn_{15}$ sample.

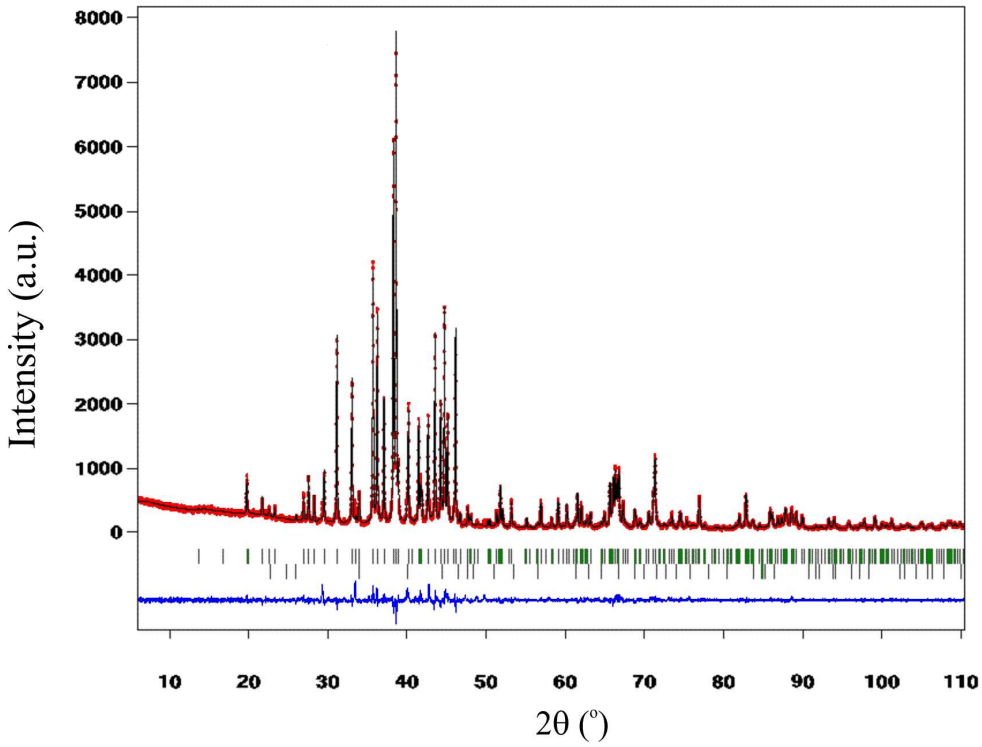

Fig. 2 Observed, calculated and difference X-ray patterns of the $Er_{15}Cu_{70}Sn_{15}$ sample (98.86% $ErCu_5Sn$, 1.14% ErCuSn).

Table 1 Atomic positional and isotropic displacement parameters ($B_{iso}\cdot10^2$ (nm^2)) of the RCu$_5$Sn compounds (R = Gd, Tb, Er, Y), space group *Pnma*.

RCu$_5$Sn	Gd	Tb	Er	Y
R (4*c*) *x* 1/4 *z*, B_{iso}	0.2526(1) 0.5625(3) 0.88(1)	0.2536(4) 0.5626(3) 0.68(9)	0.2505(2) 0.5636(3) 0.57(4)	0.2504(3) 0.5644(2) 0.75(2)
Cu1 (8*d*) *x y z*, B_{iso}	0.0770(8) 0.4982(6) 0.3076(1) 1.23(1)	0.0704(5) 0.4979(8) 0.3092(5) 0.69(1)	0.0703(6) 0.4998(1) 0.3100(2) 1.35(5)	0.0775(8) 0.5025(2) 0.3209(3) 1.04(2)
Cu2 (4*c*) *x* ¼ *z*, B_{iso}	0.4139(1) 0.0174(1) 1.42(2)	0.4153(8) 0.0157(5) 0.59(1)	0.4119(5) 0.0169(7) 0.75(9)	0.4163(9) 0.0161(3) 1.07(5)
Cu3 (4*c*) *x* ¼ *z*, B_{iso}	0.3195(3) 0.2434(3) 0.75(2)	0.3165(7) 0.2408(5) 0.93(1)	0.3143(4) 0.2414(3) 0.94(2)	0.3183(5) 0.2541(4) 0.81(3)
Cu4 (4*c*) *x* ¼ *z*, B_{iso}	0.0544(1) 0.0991(2) 1.38(2)	0.0589(7) 0.1013(6) 1.19(2)	0.0554(5) 0.0984(3) 1.03(8)	0.0526(4) 0.1043(5) 1.25(4)
Sn (4*c*) *x* ¼ *z*, B_{iso}	0.1381(1) 0.8593(1) 1.18(1)	0.1380(3) 0.8596(3) 0.93(2)	0.1388(2) 0.8602(1) 0.96(4)	0.1374(1) 0.8654(4) 1.04(2)
Reliability factors				
R_p	0.0362	0.0380	0.0599 [a]	0.0445
R_{wp}	0.0470	0.0501	0.0674 [a]	0.0663
R_{Bragg}	0.0693	0.0353	0.0419	0.0675

[a] 1.14% ErCuSn included in the refinement.

Table 2 Crystallographic characteristics of RCu$_5$Sn compounds.

Compound	Composition EPMA (at.%)	Lattice parameters (nm)		
		a	*b*	*c*
YCu$_5$Sn	Y$_{14.6}$Cu$_{70.6}$Sn$_{14.8}$	0.8205(4)	0.4980(3)	1.0497(5)
GdCu$_5$Sn	Gd$_{14.5}$Cu$_{70.5}$Sn$_{15.0}$	0.82406(8)	0.49935(5)	1.0586(1)
TbCu$_5$Sn	Tb$_{14.6}$Cu$_{70.9}$Sn$_{14.5}$	0.8212(4)	0.4892(1)	1.0579(3)
DyCu$_5$Sn	Dy$_{14.3}$Cu$_{71.0}$Sn$_{14.7}$	0.8197(2)	0.4966(1)	1.0548(4)
HoCu$_5$Sn	Ho$_{14.8}$Cu$_{70.8}$Sn$_{14.4}$	0.8189(6)	0.4960(6)	1.0562(5)
ErCu$_5$Sn	Er$_{14.6}$Cu$_{70.5}$Sn$_{14.9}$	0.81743(2)	0.49525(1)	1.05596(2)
TmCu$_5$Sn	Tm$_{14.8}$Cu$_{70.3}$Sn$_{14.9}$	0.8149(2)	0.4936(4)	1.0542(2)

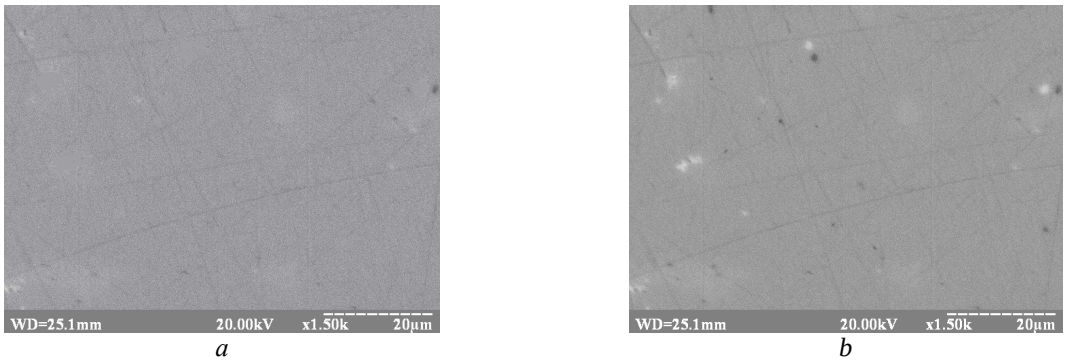

a *b*

Fig. 3 Electron microphotographs of the Ho$_{15}$Cu$_{70}$Sn$_{15}$ (*a*) and Er$_{15}$Cu$_{70}$Sn$_{15}$ (main phase – ErCu$_5$Sn; white phase – ErCuSn) (*b*) samples.

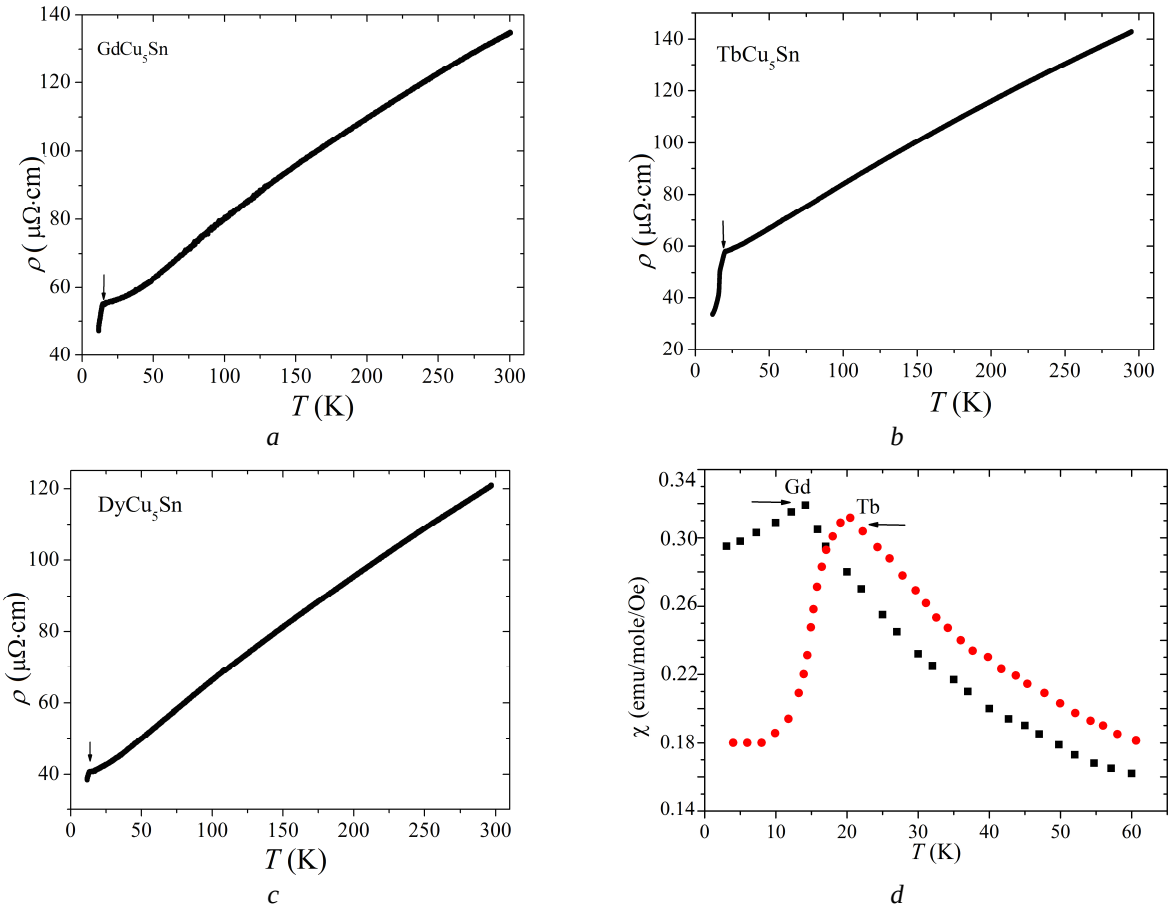

Fig. 4 Temperature dependence of the electrical resistivity of $GdCu_5Sn$ (*a*), $TbCu_5Sn$ (*b*), and $DyCu_5Sn$ (*c*) and low-temperature dependence of the magnetic susceptibility of RCu_5Sn where *R* = Gd and Tb [5] (*d*).

The resistivity of all the studied compounds increases with increasing temperature, indicating metallic type of conductivity. It worth noting that the RCu_5Sn stannides with magnetic rare earths from Gd to Tm are characterized by higher ρ values (120.7-141.3 μΩ·cm) at room temperature than the non-magnetic YCu_5Sn compound, which shows with a maximum ρ value of 86.5 μΩ·cm. The electrical transport parameters of the RCu_5Sn compounds are given in Table 3. The change of slope of the resistivity in the low-temperature part of the $\rho(T)$ dependencies, (Fig. 4*a*,*b*,*c*) observed for the $GdCu_5Sn$, $TbCu_5Sn$, and $DyCu_5Sn$ compounds, is connected with magnetic ordering (Table 3). Fig. 4*a*,*b*,*d* demonstrates the correlation between the change of slope of the resistivity plots and the magnetic transition temperatures revealed by magnetization *vs.* temperature plots for the $GdCu_5Sn$ and $TbCu_5Sn$ compounds. There is good agreement between the ordering temperatures determined from the magnetization and from the resistivity measurements (Table 3). Unfortunately, the temperature range studied here was insufficient to confirm the transition temperatures of the $HoCu_5Sn$ and $ErCu_5Sn$ intermetallics. In the temperature region above ~25 K (above the transition temperatures of the compounds with Gd, Tb, and Dy) the temperature dependence of the resistivity of all the RCu_5Sn stannides is nearly linear, which indicates a prevailing mechanism of phonon scattering.

3.3. DFT modeling

DFT modeling was carried out for the YCu_5Sn compound. The distribution of the total density of electronic states (DOS) shows the absence of an energy gap at the Fermi level, confirming metallic type of conductivity in this material (Fig. 6). Analysis of the partial DOS distribution shows that the Cu atoms are mainly represented by *d*-states in the valence band (in the form of two overlapping peaks) in the energy range from -2 to -4 eV. Both the *s*- and *p*-states of the Sn atoms are located in the valence band in the ranges -10 to -8 eV and -7 to 0 eV, respectively. The *p*-states of Sn at -4 eV mainly overlap with *d*-states of Cu1 and Cu2 atoms. The partial DOS of the Y atoms shows that the *d*-states are located in the conduction band. The occupied *d*-states in the valence band overlap with *d*-states of Cu atoms at -3 eV and with *p*-states of Sn electrons at -1 eV.

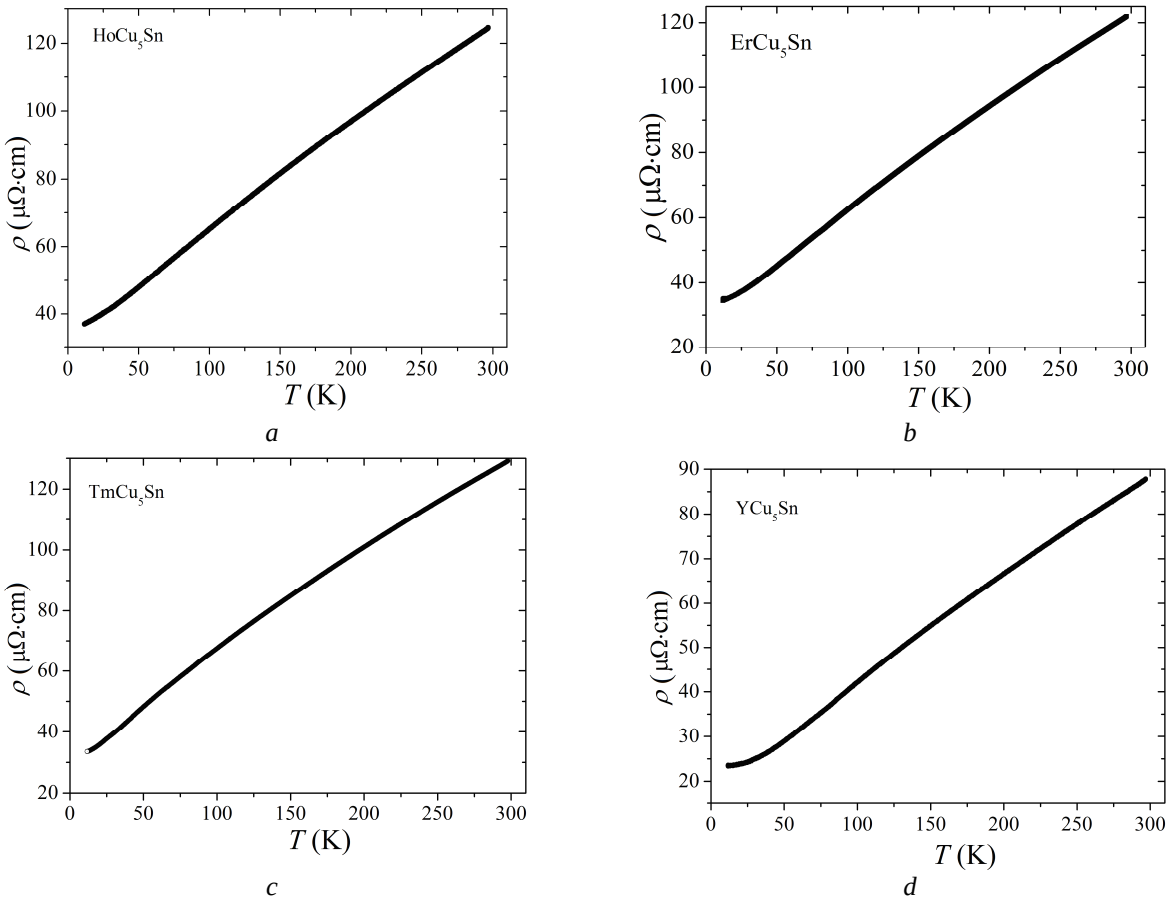

Fig. 5 Temperature dependence of the electrical resistivity of $HoCu_5Sn$ (*a*), $ErCu_5Sn$ (*b*), $TmCu_5Sn$ (*c*), and YCu_5Sn (*d*).

Table 3 Parameters of the temperature dependence of electrical resistivity for different RCu_5Sn compounds and Néel temperatures from the literature.

Compound	$\rho_{290\ K}$ (μΩ·cm)	$\rho_{11\ K}$ (μΩ·cm)	T_{ord} (K)	T_N (K) [5]
YCu_5Sn	86.5	23.2	–	–
$GdCu_5Sn$	132.7	47.2	14.6	14.0
$TbCu_5Sn$	141.3	33.6	20.1	20.5
$DyCu_5Sn$	113.4	38.5	14.0	13.0
$HoCu_5Sn$	122.7	37.2	– [a]	5.0
$ErCu_5Sn$	120.7	34.2	– [a]	1.8
$TmCu_5Sn$	127.0	34.5	–	–

[a] limit of measurement of the electrical resistivity: 11 K

Since the valence band is formed by Cu and Sn atoms, and the conduction band by Y atoms, the intermetallic compound can be considered to be polar with anionic $[Cu_5Sn]^{n-}$ and cationic $[Y]^{n+}$ sublattices. The distribution of the electron localization function (elf) shows spherical localization around the Y atoms (Fig. 7). Some electron localization between Sn and Cu1/Cu2 atoms is also observed. Such an elf distribution is in good agreement with the conclusions on bonding drawn from the analysis of the DOS. Low elf values (0.32 for the presented isosurface) show, in general, that covalent bonding is weak, and that mainly metallic/ionic distribution is present.

4. Conclusions

A series of the RCu_5Sn compounds, where *R* is Y, Gd-Tm, was studied, performing structural refinements and electric resistivity measurements. The crystal structure analysis showed ordered structures of the structure type $CeCu_5Au$ for the selected representatives of the RCu_5Sn series (Y, Gd, Tb, Er).

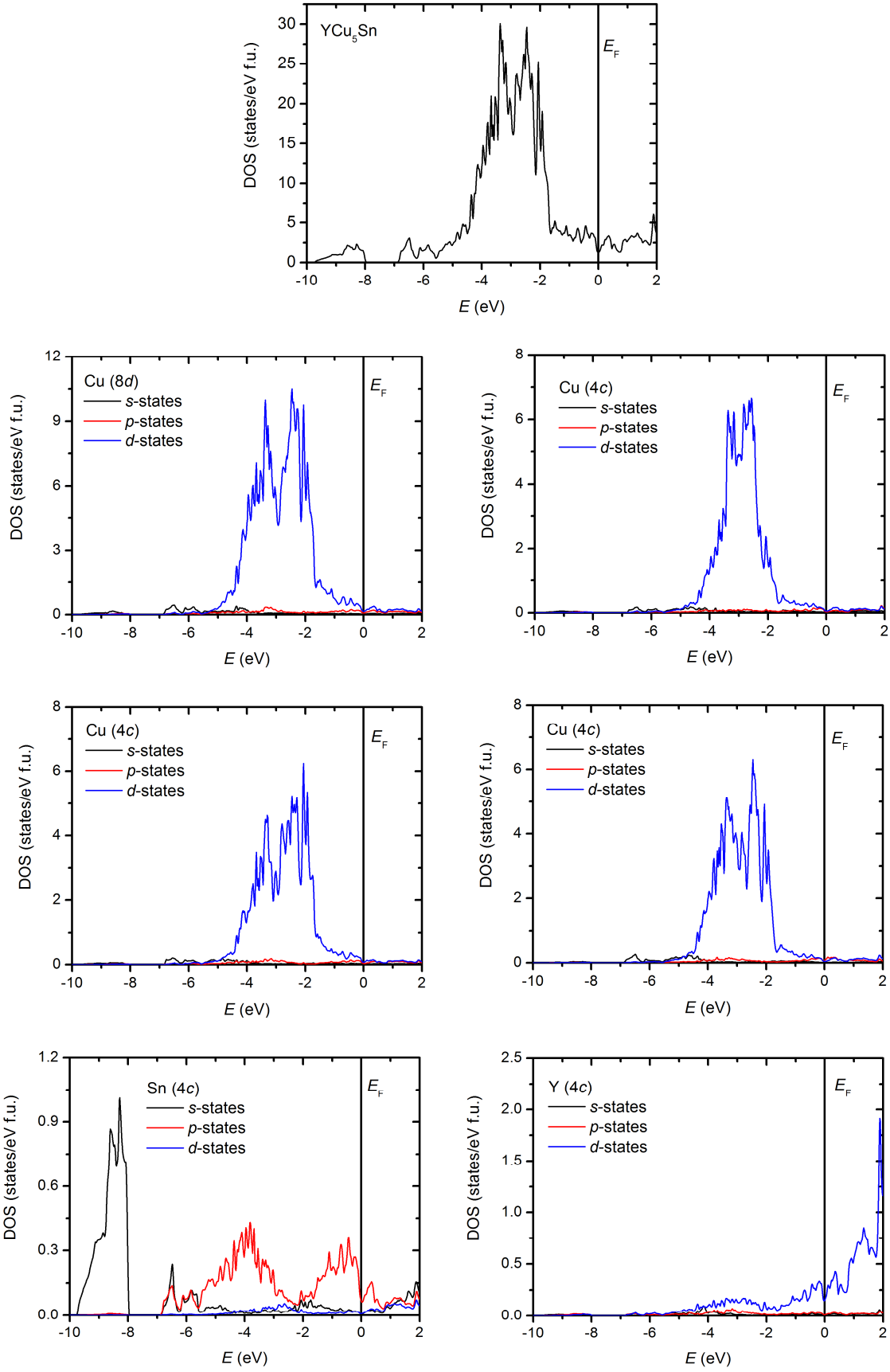

Fig. 6 Distribution of the total and partial density of states for YCu_5Sn; the Fermi level is shifted to 0 eV.

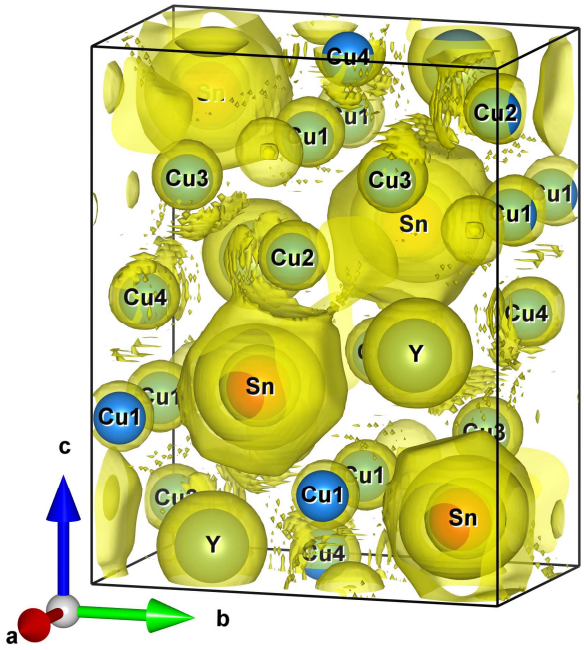

Fig. 7 Isosurface of the electron localization function at 0.32 for YCu$_5$Sn.

The electrical resistivity data indicated metallic type of conductivity for all the studied stannides. The magnetic ordering observed earlier for the GdCu$_5$Sn, TbCu$_5$Sn, and DyCu$_5$Sn compounds was confirmed by the electrical resistivity measurements. Calculations of the total DOS of the YCu$_5$Sn stannide corroborated the metallic properties.

A comparison of the electrical transport properties of other series of R_xCu$_y$Sn$_z$ compounds, *e.g.* $R_{1.9}$Cu$_{9.2}$Sn$_{2.8}$ [18] and R_3Cu$_4$Sn$_4$ [19], with those of the RCu$_5$Sn series studied in this work, shows similar metallic conductivity with low values of the electrical resistivity at room temperature (40-120 μΩ·cm, 40-160 μΩ·cm, and 86.5-141.3 μΩ·cm, respectively). In the case of the R_3Cu$_4$Sn$_4$ and RCu$_5$Sn stannides with magnetic rare earths, the transition observed on the temperature dependence of the electrical resistivity confirmed magnetic ordering at low temperature.

Acknowledgments

The work was supported by the Ministry of Ukraine for Education and Science (grant No 0118U003609).

References

[1] R.V. Skolozdra, in: K.A. Gschneidner, Jr. and L. Eyring (Eds.), *Handbook on the Physics and Chemistry of Rare Earths*, Vol. 24, 1997, 399 p.
[2] V.V. Romaka, L.P. Romaka, V.Ya. Krajovskyj, Yu.V. Stadnyk, *Stannides of Rare-Earth and Transition Metals*, Lviv Polytech. Univ., 2015, 221 p. (in Ukrainian).
[3] V.V. Romaka, D. Fruchart, R. Gladyshevskii, P. Rogl, N. Koblyuk, *J. Alloys Compd.* 460 (2008) 283-288
[4] R.V. Skolozdra, L.P. Romaka, L.G. Akselrud, J. Pierre, *J. Alloys Compd.* 262-263 (1997) 346-349.
[5] Ya. Mudryk, O. Isnard, L. Romaka, D. Fruchart, *Solid State Commun.* 119 (2001) 423-427.
[6] M.L. Fornasini, R. Marazza, D. Mazzone, P. Riani, P. Zanicchi, *Z. Kristallogr.* 213 (1998) 108-111.
[7] M. Ruck, G. Portisch, H.G. Schlager, M. Sieck, H.V. Lohneysen, *Acta Crystallogr. B* 49 (1993) 936-941.
[8] O. Isnard, J. Pierre, D. Fruchart, L.P. Romaka, R.V. Skolozdra, *Solid State Commun*. 113 (2000) 335-340.
[9] L. Akselrud, Yu. Grin, *J. Appl. Crystallogr.* 47 (2014) 803-805.
[10] J. Rodriguez-Carvajal, *Commission on Powder Diffraction, IUCr Newsletter* 26 (2001) 12.
[11] Elk, Program package; http://elk.sourceforge.net/.
[12] J.P. Perdew, A. Ruzsinszky, G.I. Csonka, O.A. Vydrov, G.E. Scuseria, L.A. Constantin, X. Zhou, K. Burke, *Phys. Rev. Lett.* 100 (2008) 136406 (4 p.).
[13] K. Momma, F. Izumi, *J. Appl. Crystallogr.* 44 (2011) 1272-1276.
[14] L. Romaka, I. Romaniv, V.V. Romaka, M. Konyk, A. Horyn, Yu. Stadnyk, *Fiz. Khim. Tverd. Tela* 19(2) (2018) 139-146.
[15] O. Sichevych, L. Romaka, Yu. Prots, M. Bobhar, L. Akselrud, *Coll. Abstr. 21st Int. Conf. Solid Compd. Trans. Elements*, Vienna, Austria. 2018, p. 22.
[16] V. Romaka, Yu. Gorelenko, L. Romaka, *Visn. Lviv. Univ., Ser. Khim.* 49 (2008) 3-9 (in Ukrainian).
[17] L. Romaka, V.V. Romaka, E.K. Hlil, D. Fruchart, *Chem. Met. Alloys* 2 (2009) 68-74.
[18] V. Romaka, Yu. Gorelenko, L. Romaka, *Visn. Lviv. Univ., Ser. Khim.* 50 (2009) 10-17 (in Ukrainian).
[19] L. Romaka, V. Romaka, B. Kuzhel, Yu. Stadnyk, *Visn. Lviv. Univ., Ser. Khim.* 54 (2013) 136-141 (in Ukrainian).